DOI: https://doi.org/10.24297/jap.v16i1.7390

The Correlation Between Fluxes of Balmer Emission Lines of H_β and H_α and Colors of a Galaxy in VNIR Region

Layali Y. S. AL-Mashhadani [1] & Orooba J. Taresh [2]

[1] Department of applied mathematics Mälardalens University, Sweden

Email: layaleyahya@gmail.com

[2] Department of physics, College of Education for pure Science (Ibn AL-Hytham), University of Baghdad

Email: Dr.ooroba.jameel@gmail.com

ABSTRACT

We have studied the correlation between the flux and colors of a galaxy sample from SDSS, Data Release 13 as measured by the standard Balmer decrement technique in both visible and near-infrared region, covering the spectral region from (4500-8500) A^o.

We analyzed the spectral properties of the sample in the three (g, r, i) optical bands and found that the main sample tends to be redder which gives an indication that the sample has higher metallicity or older age.

We carried out the standard procedures IRAF software package to get a deeper insight into the flux in H_β and H_α wavelengths range.

We have concluded that the distribution of H- Beta and H- alpha line profiles is Gaussian in the two regions.

We found also a linear correlation between Balmer decrement (H_α /H_β) in lognormal units and the rest frame colors of the sample with the best fit of 3.4764.

Mean and root means square (rms) profiles of H_β and H_α shows a maximum peak in the red region at the radial velocity of 1000km/s and the profiles were high symmetry in this region.

Key words: Galaxies. Line profiles. Balmer decrement. Spectra

INTRODUCTION

The spectroscopic data in SDSS in identified according to the "plate" associated with each observation. There are three quantities should be specified to identify a spectrum in the survey.

i. The plate number (PLATE).

ii. Night of the observation (MJD)

iii. Fiber ID, the fiber number (1-640 for SDSS-I/ II)

Each spectrum file is stored in FITS format named by " SpPlate _ pppp_ mmmmm . Fits", where pppp are four digits of the plate number, and mmmmm are five digits of MJD number. For more details you can see:

www.sdss3.org/dr13/spectro/spectro_basic.php

Spectra of a galaxy observed by SDSS have a high resolution around 1500_ 2500 at the wavelength range from (3800_ 9200) A° and the spectroscopic calibration around 10 percent [1]. These lines are both strong lines in the optical and ubiquitous as they arise from the recombination process. As the atomic structure of hydrogen is good understood, the emission lines of the flux can be calculated and the relative flux of the lines are weakly dependent on the local conditions. The ratios have calculated the difference between the measured ratio of Balmer lines and the intrinsic values can be depended to measure the reddening of a galaxy [2]. The accurate measurement of Balmer decrement used often to measure the amount of the dust extinction attenuating the observed emission lines because of Balmer decrement are insensitive to the temperature and density of the gas in low density, dilute radiation field conditions. [3]

The sample

We have selected photometric and spectroscopic data from SDSS- Data Release 13, through submitting a query written in SQL_ language to the database archive though CAS jobs interface. SDSS database has been covered 14, 555 deg^2 of the sky. [4]

The SDSS a pair of multi _ fiber spectrographs with a fiber of 3″ in diameter with a pixel spacing in log _ wavelength (10^{-4} dex). A 120 megapixel CCD camera images 1.5 deg^2 of the sky operating with five filters, u, g, r, i, z covers the regions in ultraviolet, green, red, and two infrared.

The fibers are focuses as possible to the centers of target galaxies [5].

The flux in units of 10^{-7} erg cm^{-2} s^{-1} $A^{\circ -1}$ and wavelength _ calibrated spectra cover a range of (3800_ 9200) A˚ with a resolution of 1500 at 3800 A˚ and 2500 at 9200 A˚ .

In this work, we have studied the physical properties of H_β and H_α in the wavelength ranges in between (4800_8000_) A˚ in g, r, and i _bands at the redshift of $0.1 < z < 0.2$.

The emission lines fluxes of our sample have been calculated using MPA _ JHU spectroscopic reanalysis of SDSS [6].

Data reduction and Results

The magnitudes and Balmer emission lines in H_β and H_α regions were carried out using the standard procedures of IRAF software package.

The apparent magnitude in g, r, i _ bands need to be corrected for galactic extinction see [7].

The absolute magnitudes from SDSS have been converted to the rest frames of the sample.

Since the light moves between the filters, we need to do k_ correction from the fluxes in the three bands. This is already done in SDSS in photo Z_ table. Thus we obtained the K_ correction for the sample by Casjobs interface from photo Z table.

The fluxes have been fitted in the rest_ wavelengths range of (4800- 8000) A˚.

In the following sections, we have explained the variety of the Balmer emission lines in the three bands, the correlation between the colors and Balmer decrement, and comparison between profiles of the mean and root mean square.

Variation of H_β and H_α lines in g, r, i _ bands

The photometric properties of the galaxy in the three optical bands of g, r, i, is shown in the spectrum in (Fig. 1). The spectrum covers the range from (4800_8000) A˚. The redshift of the sample galaxy of 0.1 < z < 0.2 is indicated in the bottom of the figure and the emission lines are marked also.

The spectrum covers the regions from the visible to near-infrared (NIR) according to these three optical bands in the ugriz_ photometric system.

The spectrophotometric features of our sample are summarized in table 1

Table1 The spectrophotometric features of the sample

Band	Magnitude limit	RPCA(RMS)	ECW	FWHM
g	22.2	0.8 %	4686 A^{o}	138.7 nm
r	22.2	0.8 %	6165 A^{o}	124.0 nm
i	21.3	0.7 %	7481 A^{o}	130.3 nm

The table contains the magnitude limits in g, r, i bands, the relative photometric calibration accuracy (RMS) as measured by Padmanabhan et. al. 2008 [8], the effective central wavelength, and the fall width at half maximum.

We note that the strong broad Balmer lines of the hydrogen are identified in the three bands of the spectrum. These strong emission lines as H_{β} and [OIII] near 5000 A^{o} in g- bands. Other strong emission lines as H_{α} and [NIII] near 6600 A^{o} in r_band.

The spectrum also shows some weak low ionization emission lines. These lines are produced by ionized and hot gas which often seen in the regions where the stares are forming. This is not within the field of interesting of this work. We focused on H_{β} and H_{α} emission lines only.

In addition, the sample galaxy is displayed a red color indication of old stellar population. This is clear as a sharp decline of the flux around λ = 5000 A^{o} and λ = 6600 A^{o} and this is characterized by absorption lines whose strength is a good indicator to study the age and metallicity of the galaxy

(Fig. 1) Shows also the luminosity distributions of the main sample in the three optical bands are approximately similar. The main sample is brighter than Mg < 20 with a median brightness in g-band of Mg = 18.11, Mr < 19 with a median in r_band of Mr = 17.11, and also brighter than Mi < 17 with a median brightness in i_band of 16.6.

We notice that it is no longer different between the brightness of the main sample in the three bands.

According to Wien's law, the hotter objects emit radiation and produce peaks at shorter wavelengths range, hence they will be bluer, while the cooler objects emit radiation and produce peaks at longer wavelengths range, hence they will be redder [9].

We conclude that our sample tends to have redder color, which gives an indication that the sample has higher metallicity or old age.

The luminous red galaxies are a good indicator to classify the galaxies based on luminosity-color relation [10]

To get a deeper insight into the fluxes of H_β and H_α, we plotted the line profile for each line separately. We have plotted a histogram of 20 bins of equal length (lower part of Fig. 1). The distribution of the profile as clear in the green dash line is Gaussian in the two regions.

We refit the distribution using (Specfit function in IRAF) in order to reassemble both H_β and H_α emission lines. The result of the two fitting is shown in the red-solid curve in the plot. It can be seen that the broad emission lines of the H_β and H_α shows a good inspection by Gaussian 3 with two peaks in H_β and three peaks in H_α regions. The fitting for H_β line is less uncertain. This is because of its lower flux in g_band comparable with Hα emission line in i_band.

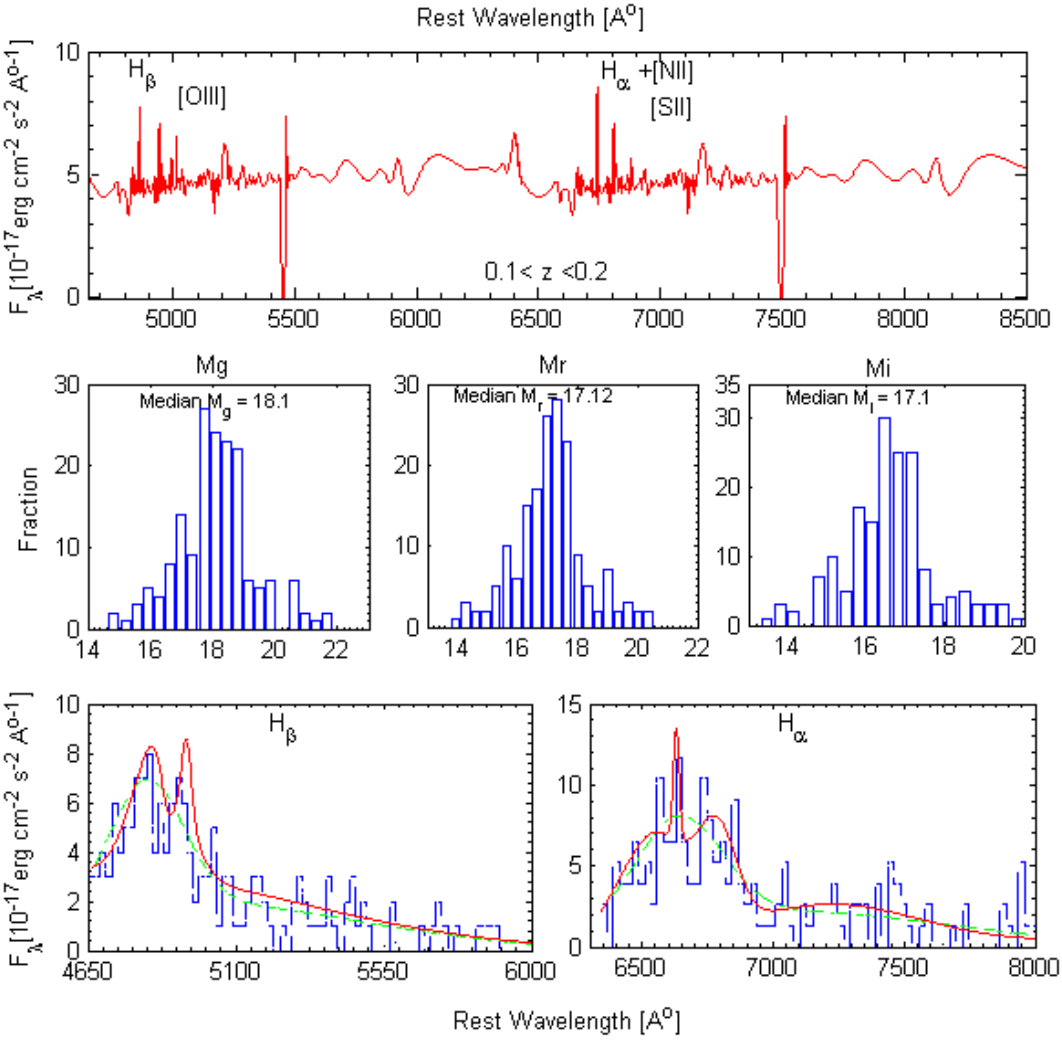

Fig. (1): The spectrum of the galaxy in the visible/near-infrared (upper panel). The middle panel shows the luminosity distributions of the galaxy in g, r, i _ bands. The lower panel shows H_β and H_α profiles on the left and right respectively.

The correlation between the flux ratio F (H_α / H_β) and the colors

The flux ratio very tied to the optical color of the galaxy. We have studied the colors distribution of the main sample in the three bands. The two emission lines that affect the broadband colors are H_β and H_α. The color distribution of ***g - r*** and ***r - i*** in the rest frame of the sample is Gaussian as shown in the upper panel of (Fig. 2), mean of ***g - r*** and ***r - i*** colors are equal and the presence of H_β and H_α keeps the average of the colors to be relatively red .

In the same figure, we have explained the correlation between the flux ratios of Balmer decrement and the colors. See the lower panel of (Fig. 2). The error bars with hexagram explains median of the fluxes in each band of a histogram of 10-bins of equal length.

We have done a linear fit as shown in the dash-red line and found that the best linear fit relation is ***y = 0.2376 (g-r) + 3.4764*** and a standard deviation of 0.6922. It is clearly good that both colors give the same constraints.

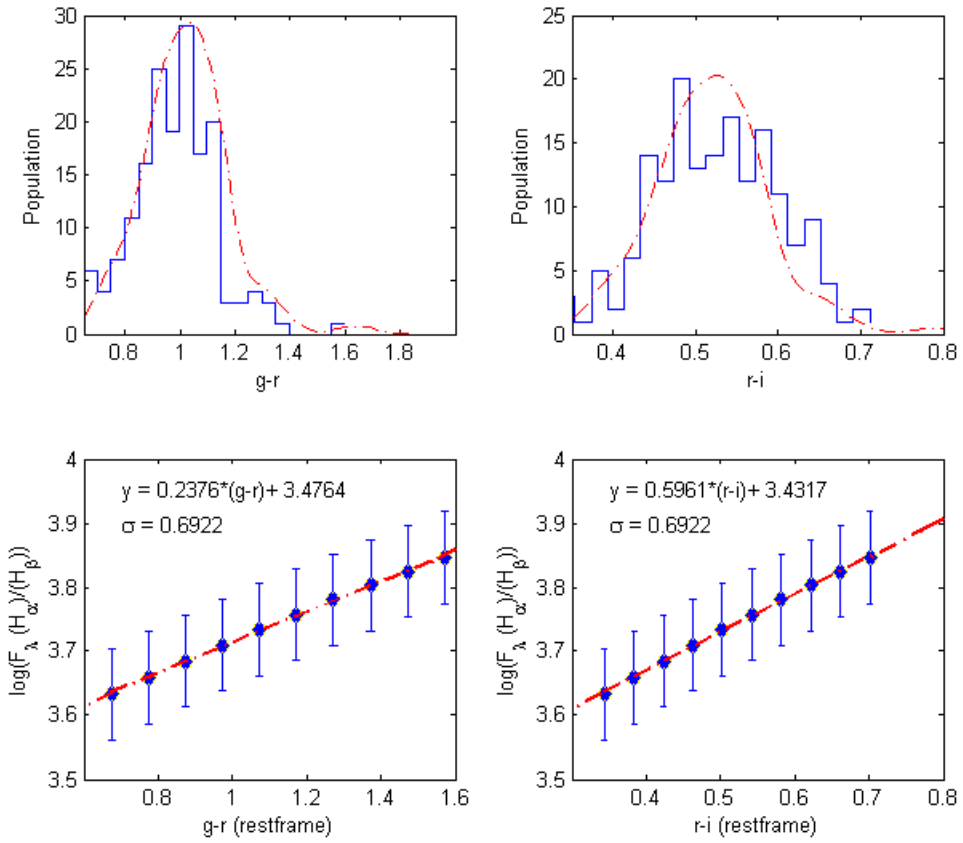

Fig. (2): Upper panel shows the color population of the galaxy. (g-r) on the left and (r-i) on the right. The lower panel shows the median of the continuum fluxes F_λ ((Hα)/(H_β)) versus the restframe g-r color (left) and r-i color(right).

Mean and root mean square (rms) profiles of H_β and H_α

Studying the shape of line profiles of the mean and rms of the H_β and H_α with the radial velocity gives us a good inspection about a variation of the emission lines in the interesting part of the spectrum.

(Fig. 3) explains the mean and rms profiles of H_β and H_α per unit wavelength. The variable part of the two profiles at radial velocity larger than 1000km/s and less than 6000 km/s corresponding to the strong emission

lines. While the constant part of both profiles is at radial velocity larger than 6000km/s corresponding to weak emission lines.

The fluxes in a unit of 10^{-17} erg cm^{-2} s^{-1} A^{o-1}. It is clear also that the maximum red peak of the profile at a radial velocity around 1000km/s in the red region of the spectrum.

The variable part of the profiles are red asymmetry after the maximum peak of the radial velocity of 1000km/s and the fluxes are decreasing when the radial velocity increasing. This is an indication of the colors variation in the three bands and the main sample is brighter in (***g-r***) comparable with (***r-i***) color. It can be seen also that mean of the flux of H_β emission line is lower than the mean flux of H_α emission line due to the rapid gas motion at the high velocities.

The flux ratio of Balmer decrement (H_α/H_β) at the range of the given velocity gives an indication of the physical condition of the emitting gas at this velocity.

The lower panel of (Fig. 3) shows a linear relation between flux ratios of (H_α/H_β) with the velocity. It can be seen that the flux ratio increasing rapidly at the higher velocity levels due to the stellar emissions effect, especially for weak emission lines.

The fitting line of (H_α/H_β) appears no turning or inflections point in the velocity range. This is mean that the emitting materials do not have a turning point at this velocity range.

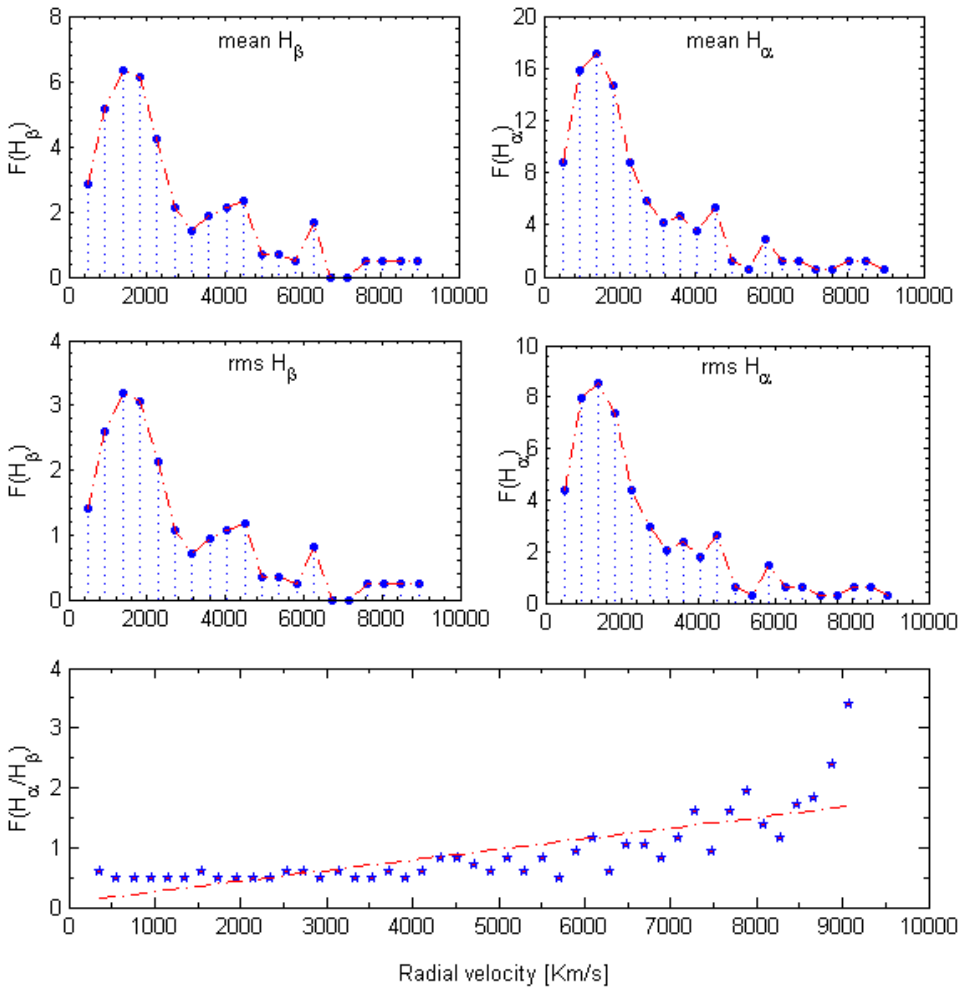

Fig. (3): The mean (upper panels) of H_β on the left and Hα on the right versus the radial velocity. The rms (middle panels) of H_β on the left and Hα on the right versus the radial velocity. The lower panel shows Balmer decrement F (H_α/H_β) versus the radial velocity.

Conclusions

We have studied the correlation between the flux and colors of a galaxy sample. We have found that the flux in different ranges of the rest wavelength varies simultaneously and changes in the shapes of the different emission and absorption lines are either strong lines near broad of H_β and H_α emission lines components in the blue-green and red regions respectively. The weak absorption lines are due to the interstellar medium which can be wrested the energy from the passing radiation.

The fluxes ratio of H-alpha and H- beta wavelength versus the rest frame colors shows a linear correlation with the best fit coefficients of Balmer decrement in lognormal units is 3.4764 and a slop of [log (flux(H_α/H_β))/$(g-r)_{rest}$] equal to 0.2376.

The mean and rms profiles of H_β and H_α shows a maximum peak at the radial velocity of 1000km/s in the red region of the spectrum and the behavior of Balmer decrement changing symmetry at the radial velocity higher than 1000 km/s. This is probably due to the ionization parameters.

We also observed that Balmer decrement has been increased at the range of the higher velocity.

References

Chris Stoughton, R., Lupton, M., Michael R., B., Scott Burles, F., Castander, A., Connolly, D., E., Joshua, F., Hennessy, R., Hindsley, et. al., Sloan digital sky survey: Early data release, The Astronomical Journal, 123:485–548, 2002 January

http://iopscience.iop.org/article/10.1086/324741/pdf

1. Claus Leitherer and Daniela Calzetti, Ultraviolet spectra of star-forming galaxies with time-dependent dust obscuration, The Astrophysical Journal, 574:114–125, 2002

   doi: 10.1086/340902

2. Brent Groves, Jarle Brinchmann1 , and Carl Jakob Walcher, The Balmer decrement of SDSS galaxies, astro-ph. CO, 2011

   https://arxiv.org/pdf/1109.2597.pdf

3. A.R. Thakar, A.S. Szalay, and J.V. Vandenberg, Data Organization in the SDSS Data Release 1, ASP Conference Series, Vol. 295, 2003

4. Alexander S. Szalay, J., Ani R. Thakar, P., Tanu Malik, J., Christopher Stoughton, J., The SDSS SkyServer – Public Access to the Sloan Digital Sky Server Data, ACM SIGMOD 2002 proceedings

   https://arxiv.org/ftp/cs/papers/0202/0202013.pdf

5. Christy A. Tremonti, T., Guinevere Kauffmann, J., Ste´phane Charlot, S., Mark Seibert, E. David J., A. , Masataka Fukugita, J., The origin of the mass-metallicity relation: insight from 53,000 star-forming galaxies in the Sloan Digital Sky Survey, The Astrophysical Journal, 613:898–913, 2004

   http://iopscience.iop.org/article/10.1086/423264/pdf

6. David J., Douglas P. and Marc Davis, Maps of Dust Infrared Emission for Use in Estimation of Reddening and Cosmic Microwave Background Radiation Foregrounds, The Astrophysical Journal, 500:525–553, 1998

   http://iopscience.iop.org/article/10.1086/305772/fulltext/

7. Nikhil Padmanabhan, D., Douglas P., J., Michael R., H., James E., M., David W., Z. , David Johnston, S., et. al., An improved photometric calibration of the Sloan Digital Survey Data, The Astrophysical Journal, 674:1217Y1233, 2008

   http://iopscience.iop.org/article/10.1086/524677/pdf

8. L. S. Sparke & J. S. Gallagher, 2007, Galaxies in the Universe: An Introduction, Second edition, Cambridge University Press

9. A. I. Shapovalova, L., A. N. Burenkov, V., D. Ilic´, A., W. Kollatschny, J., N., J. R. Valdes, J., J. Leon, A., et. al., Spectral optical monitoring of the narrow-line Seyfert 1 galaxy Ark 564, The Astrophysical Journal Supplement Series, 202:10 (22pp), 2012

   doi:10.1088/0067-0049/202/1/10